Proceedings of IMECE2007
2007 ASME International Mechanical Engineering Congress and Exposition
November 11-15, 2007, Seattle, Washington, USA

IMECE2007-43778

Exploring the basins of attraction of tapping mode atomic force microscopy with capillary force interactions

Nastaran Hashemi[a], Mark Paul[a], Harry Dankowicz[b]
[a]Department of Mechanical Engineering
Virginia Polytechnic Institute and State University
Blacksburg, VA 24061
[b]Department of Mechanical Science and Engineering
University of Illinois at Urbana-Champaign
Urbana, IL 61801

We numerically explore the nonlinear dynamics of the oscillating cantilever tip in tapping mode atomic force microscopy. The cantilever dynamics are determined by complex force interactions between the sample surface and the oscillating cantilever tip which are dominated by attractive, adhesive, and repulsive contributions depending on the instantaneous position of the cantilever. We use a model proposed by Zitzler et al that includes a capillary force interaction due to the thin film of water that covers all surfaces as a result of ambient humidity. As the cantilever approaches the surface a meniscus is formed and as the cantilever retracts this water layer forms a neck and eventually breaks. This introduces hysteresis since the formation of the meniscus and the breaking of the water neck occur at different spatial locations during an oscillation of the cantilever. Using forward-time simulation with event handling techniques tailored for situations with rapid changes in force interactions we find three classes of steady-state dynamics: (i) a branch of solutions with periodic dynamics and large amplitude of oscillation; (ii) a branch of solutions with periodic dynamics and small amplitude of oscillation; (iii) windows of irregular aperiodic dynamics. We quantify the global basins of attraction for these solutions by performing a large set of numerical simulations over a wide range of initial conditions. Our findings provide a useful framework for further studies interested in controlling these dynamics.

I. INTRODUCTION

Atomic force microscopy (AFM) has revolutionized surface science with its ability to generate topographical mappings with atomic scale resolution [1–4]. Tapping mode AFM offers advantages in surface topography when compared to contact and non-contact modes. In tapping mode the cantilever probe makes only intermittent contact with the sample and, as a result, this can be used to reduce sample destruction during measurement. Consequently, the tapping mode has been widely employed to study compliant materials and soft nanostructures [2, 4]. In typical operation the AFM cantilever oscillates near its natural frequency in proximity to the sample while a feedback control system keeps the oscillation amplitude constant [5].

The interaction forces between the AFM tip and the sample are discontinuous, nonlinear, and hysteretic. As a result the cantilever dynamics are difficult to model, analyze, and study. For example, for a given set of parameters there often exist multiple solutions [4–8]. As a result, the oscillating AFM cantilever can switch between solutions and it is often the case that one solution will have a larger impact velocity which can be detrimental to the sample [4].

The interaction forces between the tip and sample are very complex and are described by a growing and substantial literature [5, 7, 9–13]. Earlier work has shown that during the operation of a tapping mode AFM two branches of stable oscillations are found as one varies the drive frequency [5, 7, 14, 15]. The bistable behavior is due to the attractive and repulsive tip sample interactions. Garcia and San Paulo [5] investigated the cantilever dynamics as the equilibrium separation between the probe and sample was varied. This permitted an exploration of the attractive and repulsive regimes and the transition between multiple stable solutions. Zitzler et al. [7] explored the role of capillary forces resulting from a thin layer of water covering both the sample and cantilever due to humidity in the surrounding air.

The objective of this research is to quantify the dynamics of AFM cantilevers in tapping-mode operation with the inclusion of capillary force interactions. We are interested in determining all the possible steady state solutions and in approximating the basins of attraction of these attractors. Eventually we would like to build an understanding of how these attractors change as system parameters are varied. Of particular interest is the variation of the equilibrium separation of the cantilever from the surface during surface scanning.

We conduct this study by performing a large number of forward-time simulations using event handling techniques tailored for use with discontinuous systems. Similar studies have been performed in the absence of the capillary force and have uncovered the coexistence of multiple steady state solutions with complex basins of attraction [4, 16]. It is not clear beforehand if these findings remain with the inclusion of the capillary fluid layer that is present in experiment.

The deterministic character of the equation of motion

requires that when a steady state attractor is found, the AFM cantilever oscillates there, independent of the extent of its basin of attraction. However in any experiment or numerical simulation, small perturbations can influence the dynamics significantly. For AFM experiments, the perturbations can be due to the mechanical and thermal noise [17] or due to the finite time response of the feedback electronics [6]. For AFM simulations, small perturbations exist due to the particulars of the numerical scheme as well as round-off error. It is very important that the numerical approach used is specifically tailored for systems with rapidly changing vector fields as we discuss here.

II. MODELING THE TAPPING MODE ATOMIC FORCE MICROSCOPE

To numerically simulate the dynamics of a tapping mode atomic force microscope, we use a spatially lumped model available in the literature [5, 7]. Figure 1 shows a schematic of the AFM treated as a lumped mass oscillating near a sample located to the right. The shaded region indicates the thin water layer that covers both tip and sample.

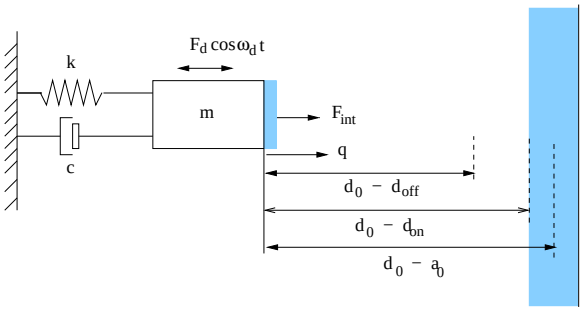

FIG. 1: A schematic of the point-mass model used to represent an AFM cantilever oscillating in tapping mode near a sample located on the right. The cantilever is represented as a mass m attached to a spring k and a damper c. The mass is driven by an oscillating external force of magnitude F_d and frequency ω_d. In our notation, q is the amplitude of oscillation, d_0 is the equilibrium tip-sample separation, d_{off} is where the capillary force turns off, d_{on} is where the the capillary force turns on, and a_0 is the intermolecular distance. The interaction force between the cantilever and surface is F_{int}. The shaded region represents the thin water layer absorbed to both the cantilever and the sample surface.

The corresponding equation of motion is a nonlinear, second order ordinary differential given by,

$$m\ddot{q} + c\dot{q} + kq = F_d \cos\omega_d t + F_{\text{int}}, \tag{1}$$

where q is the instantaneous position of the mass, m is the effective mass, k is the spring constant, and c is the damping coefficient. Excitation of the mass motion is achieved through the imposition of a sinusoidally imposed force with amplitude F_d and angular frequency ω_d. F_{int} is the tip-sample interaction force which depends on the excursion q of the tip relative to a reference level (at a distance d_0 from the sample surface) and its past motion as shown in Fig. 1. The interaction force includes attractive, repulsive, and capillary contributions.

The attractive forces are due to van der Walls interactions which are commonly estimated by considering the cantilever tip as a sphere near an infinite flat surface [18]. Assuming a sphere of radius R the attractive van der Waals force F_{vdw} is given by,

$$F_{\text{vdw}} = \frac{HR}{6(d_0 - q)^2}, \qquad d_0 - q > a_0 \tag{2}$$

where H is the Hamaker constant, $d_0 - q$ is the instantaneous tip-sample separation, and a_0 is the intermolecular constant. Using the Derjaguin-Muller-Toporov (DMT) contact model [18] yields the following expression for the intermolecular distance, $a_0 = (H/24\pi\gamma_{sv})^{1/2}$, where γ_{sv} is the surface energy of the tip and sample.

When the cantilever tip penetrates into the substrate surface, $d_0 - q < a_0$, there arises a repulsive force. Again using DMT theory this repulsion interaction is given by [4],

$$F_{\text{rep}} = -\frac{4}{3}E^*\sqrt{R}(a_0 - d_0 + q)^{3/2}, \qquad d_0 - q \le a_0, \tag{3}$$

where E^* is the effective Young's modulus.

The cantilever tip and sample are often covered by a thin film of water of depth h due to ambient humidity [7, 19]. As the cantilever approaches the surface it will make contact and penetrate into this water layer and continue towards the sample surface. The separation at which the approaching cantilever makes contact with the water is called d_{on}. Upon retracting away from the surface the water will form a meniscus and neck until this too breaks. The distance upon which the water layer releases from the retracting cantilever is called d_{off}. Throughout the time where the cantilever is in contact with the water there will be a force interaction that is called the capillary force which has been modelled as [7],

$$F_{\text{cap}} = \frac{4\pi\gamma_{H_2O}R}{1 + (d_0 - q)/h} \tag{4}$$

where γ_{H_2O} is the surface energy of water. For separations $d_0 - q \le a_0$, the capillary force is assumed to be constant by replacing the $d_0 - q$ with a_0 in Eq. (4). The capillary force is a hysteretic interaction force and as expected $d_{\text{off}} > d_{on}$. Furthermore, the capillary force is dissipative and represents the only nonconservative contribution considered.

To describe the dynamics of the cantilever tip, we recast Eq. (1) as an autonomous system of first order ordinary differential equations,

$$\dot{\mathbf{x}}(t) = \mathbf{f}_i(\mathbf{x}(t)) \tag{5}$$

where $\mathbf{x}$ is a three-dimensional state vector given by,

$$\mathbf{x} = \begin{pmatrix} x_1 \\ x_2 \\ x_3 \end{pmatrix} = \begin{pmatrix} q \\ \dot{q} \\ \omega_d t \mathrm{mod} 2\pi \end{pmatrix} \tag{6}$$

and q and $\dot{q}$ are the instantaneous position and velocity of the tip and $\phi = \omega_d t \mathrm{mod} 2\pi$ is the phase of the drive. The vector field is given by,

$$\mathbf{f}_i(\mathbf{x}) = \begin{pmatrix} x_2 \\ m^{-1}\left(F_d \cos x_3 - c x_2 - k_1 x_1 + F_{\mathrm{int}}(x_1, i)\right) \\ \omega_d \end{pmatrix}, \tag{7}$$

where i represents an index variable that indicates one of three possible instantaneous states of the system. Since the vector field exhibits discontinuous changes this is called a *hybrid dynamical system*. The interaction force F_{int} is indexed in the following manner: when only van der Waals forces are acting $i = 0$; when van der Waals and the capillary force is acting $i = 1$; and when van der Waals, capillary, and repulsion forces are acting $i = 2$.

When the cantilever comes in contact with or releases from the water layer there is a discontinuous jump in the tip-sample interaction force. In contrast, when the cantilever contacts or releases the surface the force interaction is continuous but the gradient of the interaction force is discontinuous. In our forward-time numerical approach we use event handling techniques to solve for the dynamics up until an event occurs where the vector field changes index. The events of interest are: contact with the water layer; contact with the surface; release from the surface; and release from the water layer. After solving the dynamics up to the precise moment of the event we resume the forward-time simulation from this point with the new expression for the vector field until the next event and so on. All of our simulations have been performed using algorithms that exploit the adaptive time-stepping and event-handling capabilities available in Matlab [20].

III. RESULTS

We explore the AFM dynamics by numerically integrating forward in time Eq. (5) using the event handling just described. The system parameters are similar to the commercially available AFM discussed in [7] and are listed in Table I.

We first show the coexistence of two branches of stable periodic solutions that oscillate at the drive frequency and are distinguished by their amplitude of oscillation. In addition, we also find the existence of windows of irregular or high periodic motion. Using the following experimental protocol we performed a sweep over d_0 to generate amplitude-distance and phase-distance plots which are shown in the upper and lower panels of Fig. 2, respectively. Initially, the cantilever is driven at its resonant frequency far from the surface such that it undergoes free oscillations. Then the separation distance between the equilibrium position of the cantilever and the sample surface, d_0, is gradually decreased. After making a small change we again let the cantilever reach steady oscillations in which all transients are allowed to decay. For the high quality oscillators of interest here this can require several thousand oscillations. For the results presented here each numerical simulation is allowed to continue for 2500 oscillations of the driving force. This number is a heuristic based on the experience gained from many numerical tests.

Spring constant	k_c	27.5 N/m
Quality factor	Q	400
Resonant frequency	f_0	280 KHz
Angular resonance frequency	ω_0	$2\pi f_0$ rad/s
Amplitude of free oscillation	A_0	21 nm
Hamaker constant	H	6.0×10^{-20} J
Tip radius	R	20 nm
Frequency of driving force	ω_d	ω_0 rad/s
Effective Young's modulus	E^*	65.93 GPa
Surface energy	γ_{sv}	75 mJ/m^2
Intermolecular distance	a_0	0.103 nm
Cantilever mass	m	k_c/ω_0^2 kg
Damping coefficient	c	$m\omega_0/Q$ kg/s
Surface energy of water	γ_{H_2O}	72 mJ/m^2
Water film thickness	h	0.2 nm
Capillary force turns on	d_{on}	0.4 nm
Capillary force turns off	d_{off}	2.32 nm

TABLE I: Values of the system parameters used in the numerical simulations to explore the dynamics of a tapping mode AFM.

The amplitude plotted in the upper panel of Fig. 2 is the amplitude of the oscillating cantilever measured at the closest point to the surface and after all transients have vanished. At each separation we plot the amplitude of oscillation corresponding to the last 200 periods to illustrate any deviations from purely periodic motion. For periodic motion oscillating at the drive frequency all 200 points will fall right on top of one another and yield a single point. For more complicated dynamics however, the plotted points will show some variation in q resulting in some apparent scatter. For large separations, $d_0 \gg A_0$, the cantilever undergoes free oscillations represented by the horizontal line on the lower branch. This branch is found from a simulation that begins with a large separation, goes to zero, and then retracts back to large separation. Based upon prior work we expected there to be a nearby solution with a slightly larger amplitude. By searching around in parameter space using different initial conditions, the upper branch solution was found and followed.

We would like to highlight that our numerical simulations did not jump from one stable solution branch to another as we changed the equilibrium separation between

the cantilever and surface. This is a result of our careful use of event handling techniques which incur very little numerical perturbation to the solution. This is not necessarily the case if one uses a simple forward-time integration scheme with only an if-then type logical structure to determine the choice of vector field at some time. This is also true if one attempts to smooth the tip-surface force over spatial discontinuities. In both cases the numerical approach would introduce unnecessary errors which may be large enough to cause the solution to jump from one solution branch to another.

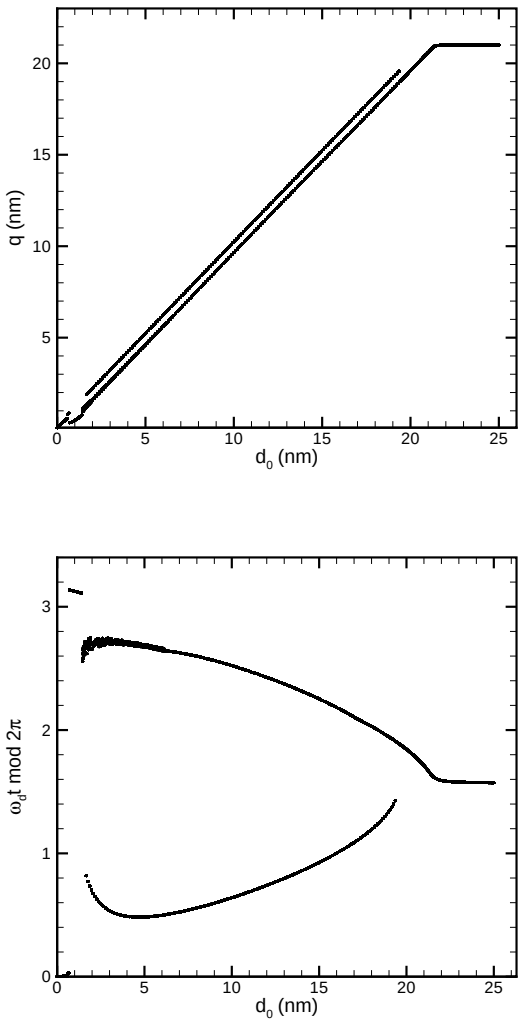

FIG. 2: Numerical results using forward-time simulation to explore the dynamics of a tapping mode AFM. (top) The variation of q at closest approach of the periodic solution with separation. (bottom) The variation of the phase with separation (phase is measured at the time as q and is shown in units of radians).

Figure 3 uses data from the same simulations to plot the minimum distance between the mass and the surface

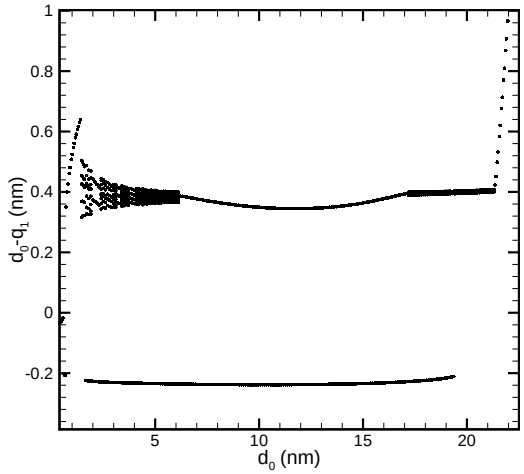

FIG. 3: Numerical results using forward-time simulation to explore the dynamics of a tapping mode AFM. The variation of $d_0 - q_{max}$ with separation. The dynamics are irregular or high periodic for windows $17.1 < d_0 < 21.3$ nm and $1.7 < d_0 < 6.1$ nm. For each value of the separation values from the final 200 oscillations are plotted.

when the mass is fully extended toward the surface given by $d_0 - q$. For the low amplitude oscillation there are two windows of separation $17 \lesssim d_0 \lesssim 21$ nm and $1.5 \lesssim d_0 \lesssim 6$ nm where the cantilever exhibits irregular dynamics.

From these simulations we have shown the existence of three steady state solutions: periodic dynamics with low amplitude, periodic dynamics with high amplitude, and irregular dynamics. The dynamics of these solutions and their relation to discontinuity induced bifurcations have been studied in detail elsewhere [21]. In order to estimate the general features of the basins of attraction for these solutions we use forward-time simulations for a wide range of initial conditions for the three different equilibrium cantilever separations shown in Table II which we will refer to these as small, intermediate, and large separations.

Case	d_0 [nm]	separation
(i)	8.5	small
(ii)	10.0	intermediate
(iii)	16.7	large

TABLE II: The three values of the equilibrium tip-sample separation d_0 used to explore the basin of attraction. The values are chosen to represent the range of separation over which it is expected that the dynamics will vary. For all simulations we have used the parameters listed in Table I, for reference $A_0 = 21$nm.

We first calculate the steady-state solutions for a one-dimensional line of initial conditions in state space. The

numerical results are shown in Fig. 4. The simulations were performed for a large set of initial conditions with finite displacement and zero velocity and phase, $\mathbf{x}(t=0) = (q_0, 0, 0)$. A grid spacing of initial displacements of $\Delta q_0 = 0.019A_0$ was used and the simulations were allowed to continue in time for 2500 oscillations of the driving force. The steady state solutions are then analyzed to determine the type of dynamics it represents. To classify the dynamics into the three groups discussed earlier we use the following convention in Fig.4: (1) represents periodic dynamics at the drive frequency with a high amplitude, (2) represents periodic dynamics with the drive frequency and low amplitude, and (3) represents irregular aperiodic dynamics which were not found for these initial conditions. The dynamics become more complicated as the separation between the sample and surface decreases. This is indicated by the top panel of Fig. 4 which shows the results for small separation and yields high and low amplitude solutions in close proximity.

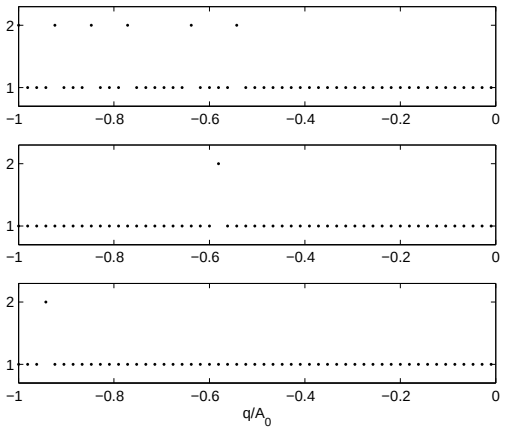

FIG. 4: A one-dimensional slice of the basin of attraction for steady state solutions for small separation $d_0 = 8.5$nm (top), intermediate separation $d_0 = 10.0$nm (middle), and large separation $d_0 = 16.7$nm (bottom). The initial conditions are chosen to be $\mathbf{x}(t=0) = (q_0, 0, 0)$ with a grid spacing of $\Delta q_0 = 0.019A_0$. In the figures the solutions are labeled on the ordinate axis as: (1) periodic with high amplitude and (2) periodic with low amplitude. Solutions with irregular steady-state dynamics were not found for these initial conditions. Each data point represents a separate simulations begun from different initial conditions.

To get an estimate of the two-dimensional basin of attraction we have also performed simulations over a large range of initial conditions in initial displacement and velocity, $\mathbf{x}(t=0) = (q_0, \dot{q}_0, 0)$. The results from these simulations are shown in the three panels of Fig. 5. Because of the computational cost of these simulations they were performed with a coarse grid of initial conditions. The grid spacing in initial displacement is $\Delta q_0 = 0.095A_0$ and the grid spacing in initial velocity is $\Delta \dot{q}_0 = 0.095A_0\omega_d$. The bottom left corner of each rectangle of Fig. 5 represents the value of the initial conditions used in the simulation. After reaching steady-state the simulation is analyzed to determine what category of dynamics it represents. A dark (blue) rectangle indicates a periodic solution with high amplitude and a light (green) rectangle represents a periodic solution with low amplitude. The simulations show a complex array of high and low amplitude periodic solutions over the range of initial conditions. Overall, we find that the high amplitude solution is more common.

The required wall-clock time for each forward-time simulation to complete the required 2500 cycles used to ensure a transient-free solution is about 30 minutes on a standard workstation running our code. This is clearly computationally prohibitive which would make a more detailed study difficult. In order to compute basins of attraction with more resolution we plan to develop and use a parallel cell-to-cell mapping approach which is much more accessible computationally [22]. The results presented here will be very useful in validating any future approaches and in quantifying any error in approximations used to speed up the calculations. For example, in the the cell-to-cell mapping approach it is important to find the required resolution in the initial condition grid that is capable of reproducing the true behavior of the hybrid dynamical system.

IV. CONCLUSIONS

We have explored the steady-state dynamics of atomic force microscopy with the inclusion of capillary force interactions. We have used forward-time simulation with event handling to carefully treat the dynamics of this hybrid dynamical system. Our numerics show the coexistence of three classes of solution: two periodic solutions with different amplitude of oscillation and solutions with irregular dynamics. We have also quantified the basins of attraction for these solutions over a range of initial conditions.

Acknowledgments: We are grateful for useful interactions with Craig Prater. We also acknowledge support from National Science Foundation CMMI Grant No. 0510044 and 0619028.

[1] G. Binnig, C.F. Quate, and C. Gerber. Atomic force microscope. *Phys. Rev. Lett.*, 56(9):930–933, 1986.

[2] N. Jalili and K. Laxminarayana. A review of atomic force microscopy imaging systems: application to molec-

ular metrology and biological sciences. *Mechatronics*, 14(8):907–945, 2004.

[3] G. Bar, Y. Thomann, and M.H. Whangbo. Characterization of the morphologies and nanostructures of blends of poly(styrene) block-poly(ethene-co-but-1-ene)-block-poly(styrene) with isotactic and atactic polypropylenes by tapping-mode atomic force microscopy. *Langmuir*, 14(5):1219–1226, 1998.

[4] R. Garcia and R. Perez. Dynamic atomic force microscopy method. *Surface Science Report*, (47):197–301, 2002.

[5] R. Garcia and A. San Paulo. Attractive and repulsive tip-sample interaction regimes in tapping-mode atomic force microscopy. *Phys. Rev. B*, 60(7):4961–4967, 1999.

[6] R. Garcia and A. San Paulo. Dynamics of a vibrating tip near or in intermittent contact with a surface. *Phys. Rev. B*, 61(20):R13381–R13384, 2000.

[7] L. Zitzler, S. Herminghaus, and F. Mugele. Capillary force in tapping mode atomic force microscopy. *Phys. Rev. B*, 66(155436), 2002.

[8] X. Zhao and H. Dankowicz. Characterization of intermittent contact in tapping mode atomic force microscopy. *Journal of Computational and Nonlinear Dynamics*, 1:109–115, 2006.

[9] Dankowicz H. Nonlinear dynamics as an essential tool for non-destructive characterization of soft nanostructures using tapping-mode atomic force microscopy. *Phil. Trans. R. Soc. A*, 364:3505–3520, 2006.

[10] S.I. Lee, S.W. Howell, A. Raman, and R. Reifenberger. Nonlinear dynamics of microcantilevers in tapping mode atomic force microscopy: a comparison between theory and experiment. *Phys. Rev. B*, 66:115409, 2002.

[11] S.I. Lee, S.W. Howell, A. Raman, and R. Reifenberger. Nonlinear dynamic perspectives on dynamic force microscopy. *Ultramicroscopy*, 97:185–198, 2003.

[12] N.A. Burnham, O.P. Behrendt, F. Oulevey, G. Gremaud, P-J. Gallo, D. Gourdon, E. Dupas, A.J. Kulik, H.M. Pollock, and G.A.D. Briggs. How does a tip tap? *Nanotechnology*, 8:67–75, 1997.

[13] K. Yagasaki. Nonlinear dynamics of vibrating microcantilevers in tapping-mode atomic force microscopy. *Phys. Rev. B*, 70:245419, 2004.

[14] J. M. T. Thompson and H. B. Stewart. *Nonlinear Dynamics and Chaos*. Wiley, 1997.

[15] P. Gleyzes, P. K. Kuo, and A. C. Boccara. *Appl. Phys. Lett.*, (58):2989–2991, 1991.

[16] M. Marth, D. Maier, J. Honerkamp, R. Brandsch, and G. Bar. A unifying view on some experimental effects in tapping-mode atomic force microscopy. *J. Applied Physics*, 85(10):7030–7036, 1999.

[17] H.-J. Butt and M. Jaschke. Calculation of thermal noise in atomic force microscopy. *Nanotech.*, 6:1–7, 1995.

[18] S. Ciraci, E. Tekman, A. Baratoff, and I.P. Batra. Theoretical-study of short-range and long-range forces and atom transfer in scanning force microscopy. *Phys. Rev. B*, 46(16):10411–10422, 1992.

[19] D. Beaglehole and H. K. Christenson. Vapor adsorption on mica and silicon: Entropy effects, layering, and surface forces. *J. Phys. Chem.*, 96:3395–3403, 1992.

[20] The Mathworks, Inc.

[21] N. Hashemi, M.R. Paul, and H. Dankowicz. The nonlinear dynamics of tapping mode atomic force microscopy with capillary force interactions. Unpublished.

[22] C.S. Hsu. A theory of cell-to-cell mapping dynamical systems. *J. Applied Mechanics*, 47:931–939, 1980.

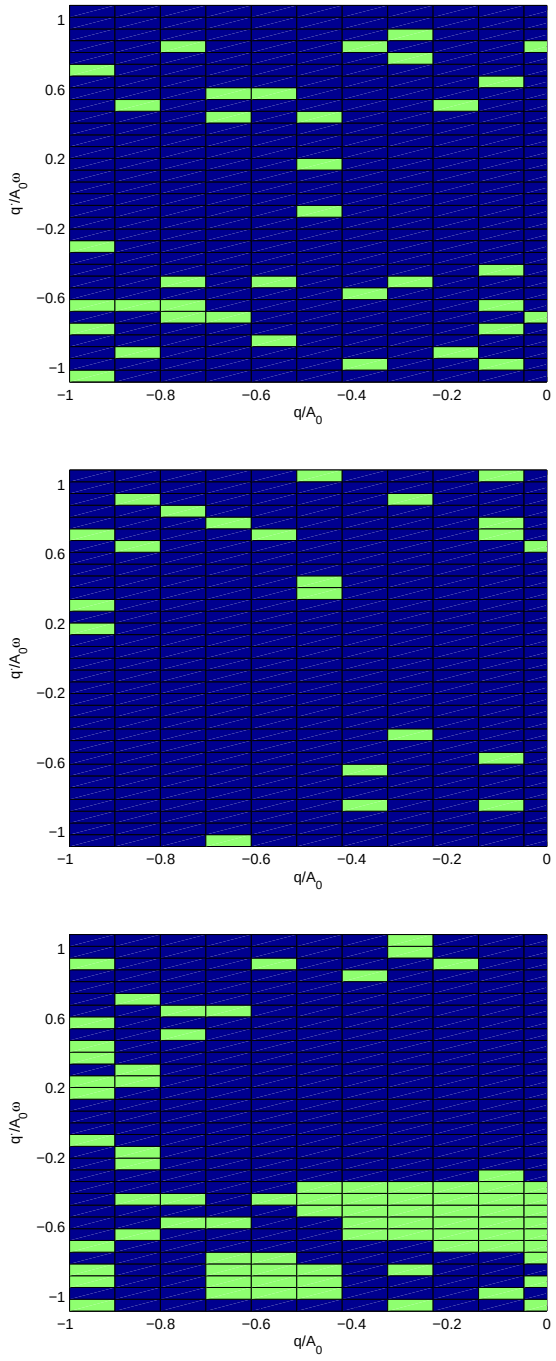

FIG. 5: Two-dimensional basin of attraction for small separation $d_0 = 8.5$nm (top), intermediate separation $d_0 = 10.0$nm (middle), and large separation $d_0 = 16.7$nm (bottom). Dark rectangles (blue, in color) represent initial conditions that yield high amplitude periodic solutions and light rectangles (green, in color) represent initial conditions that yield low amplitude periodic solutions. For the separations considered here there were no steady-state solutions with irregular dynamics.